Journal of Techniques, ISSN: 2708-8383, Vol. 5, No. 4, 2023, Pages 46-53
DOI: https://doi.org/10.51173/jt.v5i4.1503

JOURNAL OF TECHNIQUES

Journal homepage: http://journal.mtu.edu.iq

RESEARCH ARTICLE - ENGINEERING

Umbrella-Shaped Wideband MIMO Wireless Communication Antenna

Hussein Mohammed Naser[1*], Oras Ahmed Al-Ani[1], Mahmood Farhan Mosleh[1], Faiz Arith[2]

[1]Electrical Engineering Technical College, Middle Technical University, Baghdad, Iraq

[2]Faculty of Electronic & Computer Engineering (FKEKK), University Technical Malaysia Melaka (UTeM), Durian Tunggal, Malaysia

[*] Corresponding author E-mail: hussainmoh1983@gmail.com

Article Info.

Article history:

Received
07 May 2023

Accepted
19 July 2023

Publishing
31 December 2023

Abstract

A Circular Polarization (CP) Multiple Input Multiple Output (MIMO) system was used in this study with additional components for contemporary communication systems developed. There are 4 elements in the model. On the printed circuit board, each element has a dual-fed with two ports positioned at each of the four corners of smart devices (PCB). A Rogers RO3003 substrate with a dielectric structure size of (64.59 × 64.59) mm^2. geometrical shape 50-Ohm microstrip lines are used to feed the antenna ports. To accomplish polarization and variety properties, microstrip feed lines are positioned orthogonally. According to the paradigm results, the operational frequency for each port was 4.25 GHz, and the system's operating frequency was 4.23 GHz while diversity gains (DG) of the MIMO antennas were about 10, the gain was suitable (around 7 dB), and Less than 0.0001 was the envelope correlation coefficient (ECC). Additionally, the outcomes demonstrate that the MIMO system may operate in a sub-6 band that is ideal for smart device applications.

Publisher: Middle Technical University

Keywords: Diversity Gains; MIMO System; Ultra-Wideband; Envelope Correlation Coefficient; Voltage Standing Wave Ratio.

1. Introduction

The American Federal Communications Commission (FCC) announced a rule for ultra-wideband (UWB) in 2002 [1]. UWB has designated frequencies between 3.1 and 10.6 GHz. To recreate the pulse, the UWB transmitter emits a pulse with an absolute channel band less than 500 MHz [2]; the receiver then gathers the power of the signal to do so [3], having a lower amount of power spectrum density than that of receivers for other systems. UWB hence has a wide range of applications in contemporary wireless communications networks, medical imaging, and radar detection and localization systems [4]. UWB enables Wireless communications with a high data rate and good-resolution imagery in addition to its huge bandwidth [5]. Multiple input and multiple outputs (MIMO) technologies are used to boost the communication system's capacity and improve transmission quality when several antenna components are coupled at the transmitter and receiver [6]. Using such technology can solve multipath fading problems due to the wide bandwidth of UWB systems, particularly when UWB systems are utilized in wireless communication systems in conjunction with MIMO technology. On the other hand, MIMO's proximity of antenna elements may make coupling more likely [7]. Systems with MIMO are essential for modern communications.

On the other side, MIMO technology served as a representation of spatial diversity [8]. MIMO is an excellent option to examine such enhancement of the efficient spectrum without increasing input power [9]. However, due to surface currents and associated radiation, MIMO systems have a mutual coupling issue [10]. The mutual coupling problem has been approached using a variety of techniques, such as ground plane alterations [11], parasitic geometry [12], and neutralization lines [13]. Increasing the number of transceiver antennas on diversity/MIMO techniques can boost the wireless channel capacity of a wireless link in settings with significant scattering [14]. Nonetheless, MIMO antenna elements typically have very high correlation coefficients since there is limited space available for small electronic devices [15]. It is possible to demonstrate the diversity of polarization and radiation patterns using an orthogonal arrangement of microstrip feed to one another [16]. In some of the relevant studies in this field, regarding wideband applications, a novel dielectric resonator antenna (DRA) in the shape of an A stimulated by a conformal strip is suggested. The experimental findings show that the suggested DRA covers the U-NII and IEEE 802.11 bands with a 3.24–6.0 GHz (39.5%) impedance bandwidth (for S11< –10 dB). The strength of the antenna, which ranges from 5.29 to 7 dBi across the operational bandwidth, produces a somewhat consistent radiation pattern. Using the suggested wideband DRA, it also works with a dual-element MIMO system. The dual-element MIMO antenna's impedance bandwidth is 59.2% for Port 1 and 60.9% for Port 2, and over the bandwidth, more than 20 dB separates the ports from one another. Additionally, it is discovered that the MIMO antenna's diverse performance is good, with an operational band envelope correlation coefficient of less than 0.003 [17]. For use in Applications for Worldwide Interoperability for Microwave Access (WiMAX) and Wireless Local Area Networks (WLAN), In this paragraph, a simple, portable broadband MIMO antenna

Nomenclature & Symbols

PCB	Printed Circuit Board	FCC	U.S. Federal Communications Commission
UWB	Ultra-Wideband	SMA	Sub-Miniature
DG	Diversity Gain	VSWR	Voltage Standing Wave Ratio
ECC	Envelop Correlation Coefficient	MIMO	Multiple-Input and Multiple-Output
3D	Three-Dimensional	CST	Technology for Computer Simulations
ρ	Envelope Correlation Coefficient	dB	Decibel
Ω	Vertex Angle (O)		

is described. The suggested antenna uses electromagnetic band gap (EBG) technology, which is utilized to lessen the ports' mutual coupling. The antenna has a fractional bandwidth of 64.42% and operates in the frequency range of 2.01 to 3.92 GHz. It satisfies the bandwidth requirements of the WiMAX (3.2–3.85 GHz) and WLAN (2.35–2.5 GHz) bands, achieving a minimum 29 dB port isolation for the whole application band. The suggested MIMO antenna has a high diversity gain (DG > 9.8) and a very low envelope correlation coefficient (ECC 0.01). Additionally, the study shows that it has relatively little channel capacity loss (CCL), less than 0.2 bit/s/Hz. [18].

Moreover, CP antennas have become more popular recently because they have better signal propagation characteristics than Linearly Polarized (LP) antennas [19]. Nevertheless, CP can be used in conjunction with orthogonal dual-feed to provide high isolation [20]. So, the current work aims to use this approach. In numerous research, such as [21], and others, dual-polarized antennas with different slot shapes are created using a slot microstrip line. A dual-polarized MIMO system with CP is presented in this paper for use with smart devices. The Umbrella-shaped modules of the MIMO antenna are positioned on the PCB with microstrip feed lines. Moreover, there is a Square between each pair of perpendicular elements. To achieve maximal isolation, the length and width of microstrip feed lines are modified. This design has a significant return loss, a poor correlation coefficient, and a band that is essential for smart device applications.

2. Details of the Proposed Antenna

2.1. A single-antenna design

The suggested dual-polarized CP antenna configuration's schematic, which has dimensions of (24.80 x 24.80) mm^2, is depicted in Fig. 1. The Rogers RO3003 substrate has a relative permittivity of 3 and a thickness of 1.54 mm and a loss tangent of 0.001, which was used to design the antenna. Its composition includes a Geometric Shape with the addition of a Square design. The suggested feeder types consist of two orthogonally positioned Umbrella-shaped microstrip lines. Each antenna has 50 Ω connections from Sub-Miniature Version A (SMA) for the ports of antenna feeding. In this study, an Umbrella-shaped was suggested as a means of producing an elevation radiation pattern with a reasonable return loss. The suggested model strategy seeks to construct a dual-polarized antenna with a sizable return loss and a size of suitable. The values for the designed antenna arrangement model parameters are shown in Table 1.

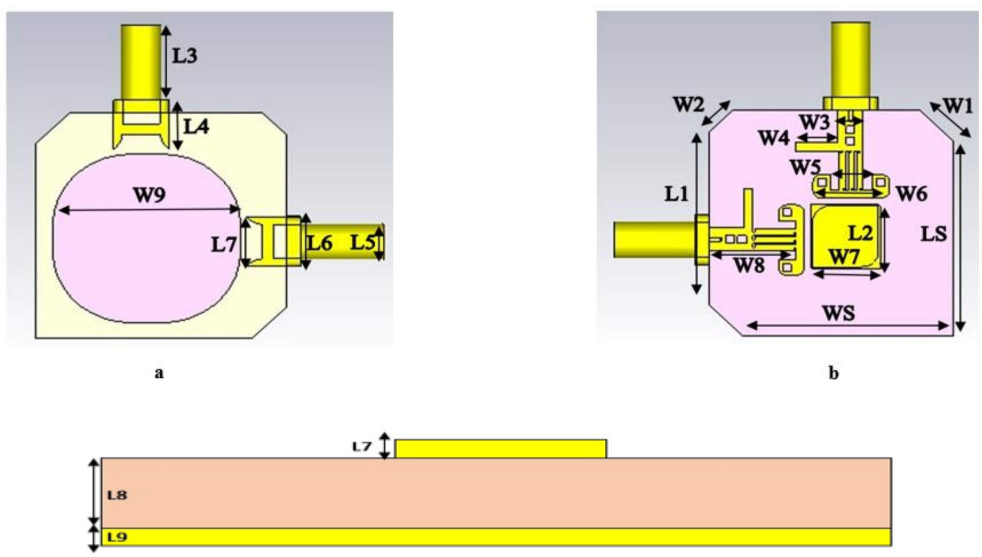

c

Fig. 1. The antenna design; a) frontal view, b) back view, and c) Side view

Table 1. Values for the antenna parameters

parameter	Value (mm)	Parameter	Value (mm)
W S	24.80	L S	24.80
W G	24.79	L G	24.79
W 1	5.66	L 1	21.92
W 2	4.07	L 2	8
W 3	3	L 3	9.52
W 4	5	L 4	6.30

W 5	5	L 5	4.54
W 6	7	L 6	6.35
W 7	8	L 7	6.35
W 8	10	L 8	64.59
W 9	21.50	L 9	7
W 10	64.59	L 10	0.03
W 11	56.59	L 11	1.54
W 12	26.71	L 12	0.03

2.2. Proposed MIMO antenna model

The MIMO antenna is built on Rogers RO3003 substrate that measures (64.59 x 64.59 x 1.54) mm^3 in total. Four separate antenna elements are combined to form the proposed MIMO antenna. The suggested porotype's slot radiators will have almost symmetrical radiation patterns and enough bandwidth to cover both the top and bottom of the PCB. Fig. 2 shows the architecture of the MIMO system.

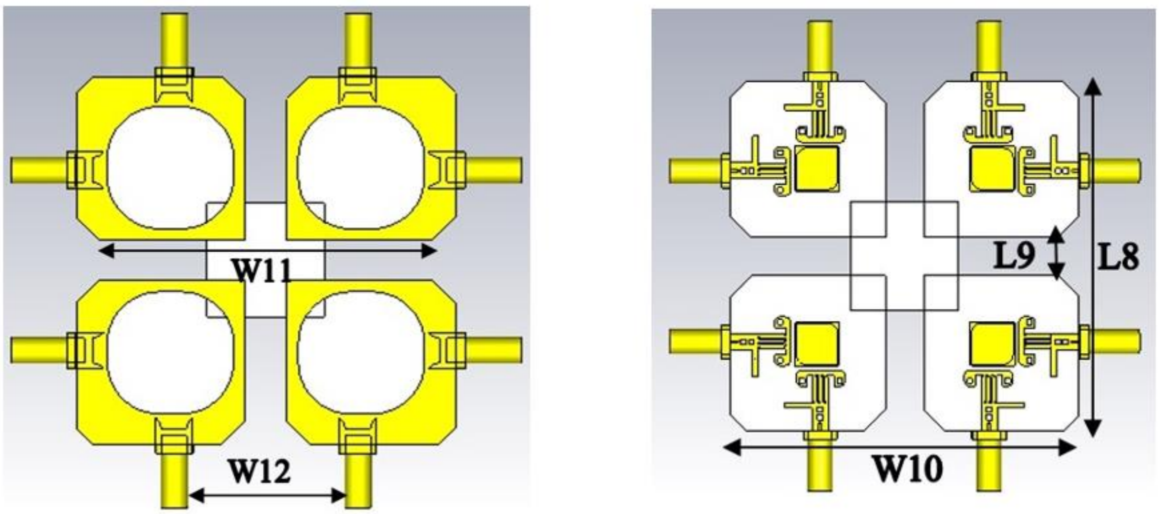

a **b**

Fig. 2. The MIMO antenna design; a) frontal view, and b) back view

3. The Simulation's Findings

CST STUDIO 2019 simulates the suggested MIMO and single model to evaluate their performance. The final suggested concept was the product of a lot of tries with varied proportions that led to the creation of such a model. To get the greatest performance, the width, length, and PCB dimensions of the microstrip-line feeder were all changed.

3.1. Simulation of a single antenna

Fig. 3 shows the return loss (-30.5 dB) and isolation of the proposed single antenna at the resonance frequency of 4.25 GHz, the operating frequency range is from 3.78 to 6.14 GHz at (-10 dB). While the suggested two-port antenna's S12 and S21 curves are shown in Fig. 4. Also observed are S12 and S21 at <-59.6 dB. The value of the two antennas' mutual coupling is consequently relatively low because the two ports are independent of one another.

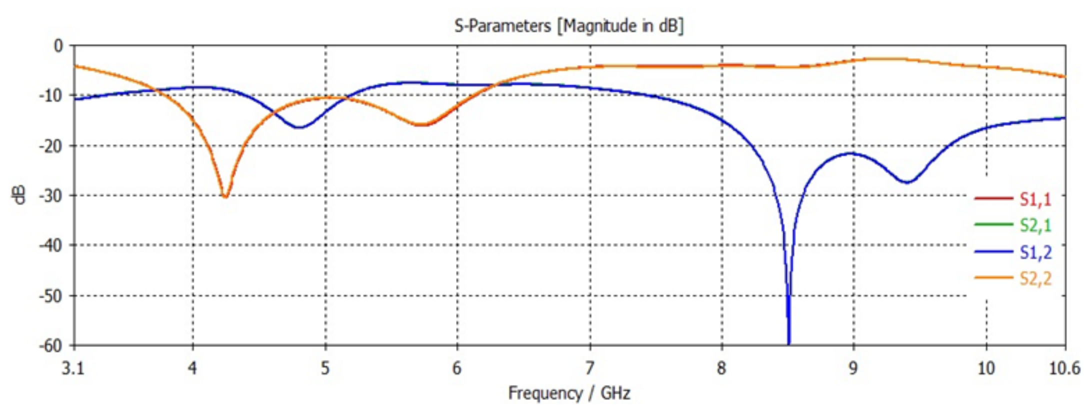

Fig. 3. Details of S-Parameter for a single antenna

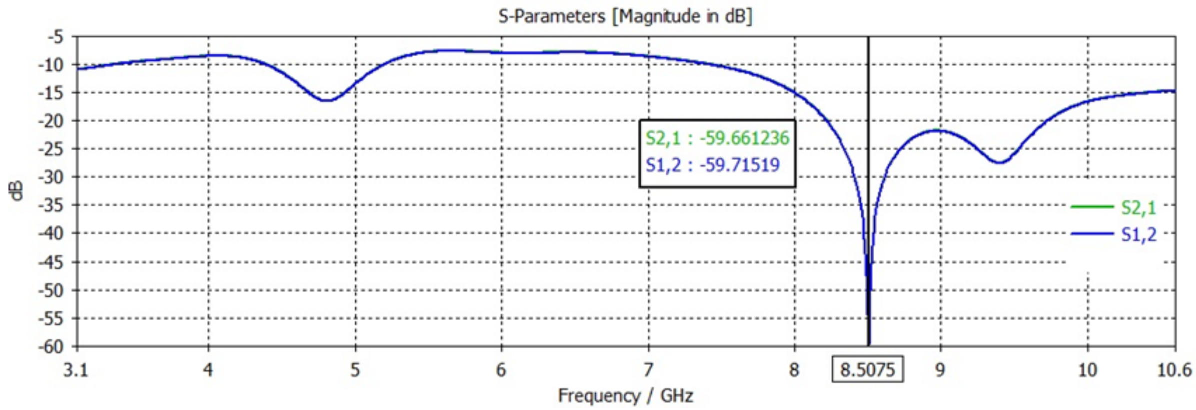

Fig. 4. The mutual coupling coefficient for a single antenna

The voltage standing wave ratio (VSWR) is shown in Fig. 5 for the feature of the proposed antenna. The calculated value of VSWR at operating frequency was 1.03 that less than 2 dB, which is consistent with [22]'s description of its condition.

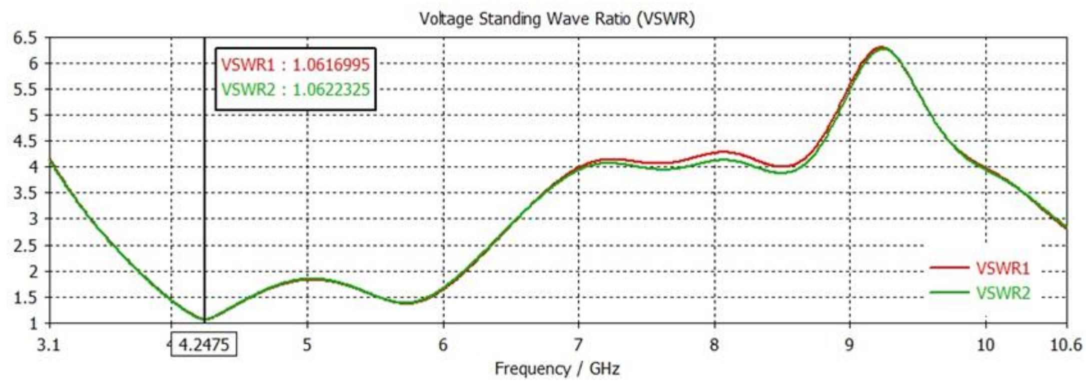

Fig. 5. The single antenna's VSWR

Fig. 6 illustrates the 3D radiation pattern that was seen at the operating frequency, Port 1 emits radiation in all directions along the XZ plane. Port 2 shows along the YZ plane an omnidirectional radiation pattern in comparison.

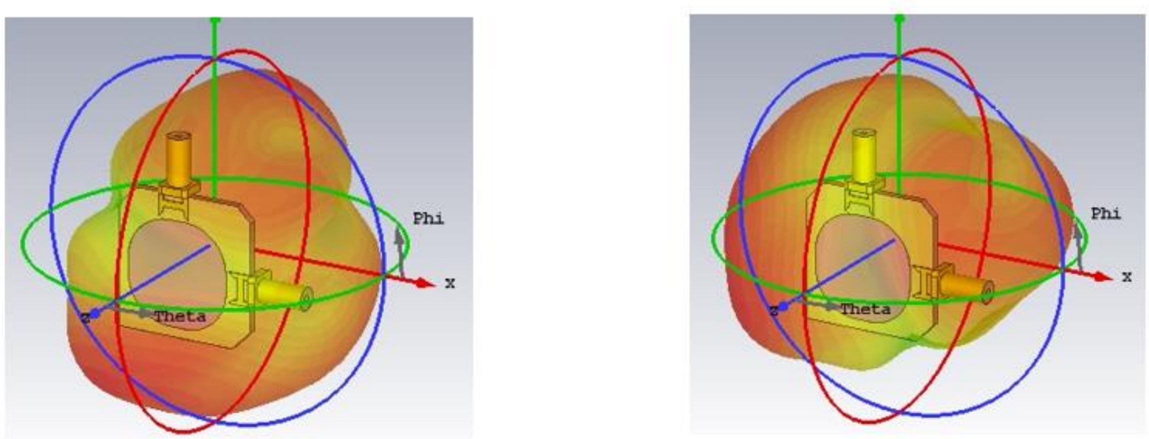

a b

Fig. 6. The dual polarized radiation's 3 dimensional; a) port_1 and b) port_2

3.2. Simulation of a proposed MIMO antenna

The MIMO model simulation addresses three performance criteria: Radiation patterns, diversity performance, and S-parameter. In regards to the S-Parameters, the desired frequency range is shown in Fig. 7. The suggested MIMO model has good isolation properties, a suitable impedance bandwidth of 2.33 GHz (3.77 - 6.1) GHz, and good S-parameters.

The suggested MIMO system's VSWR performance across all ports, as shown in Fig. 8, shows that the value is below 2.

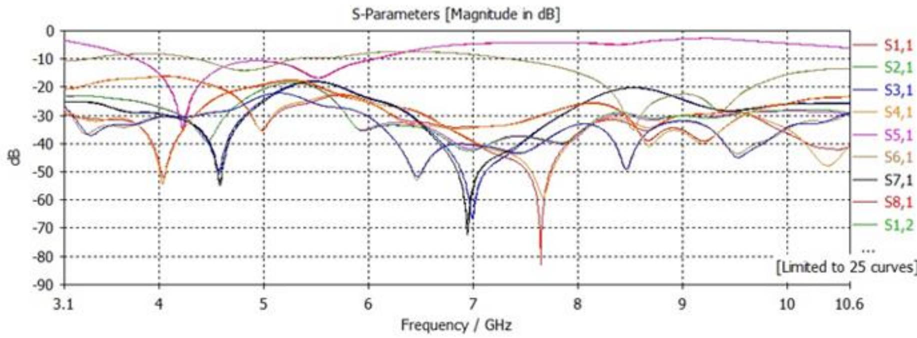

a

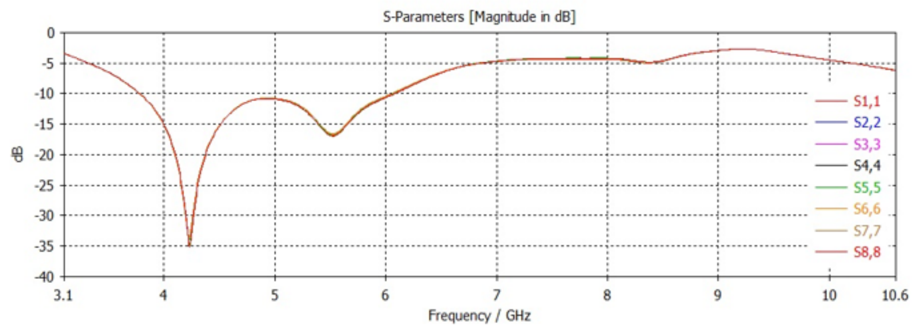

b

Fig. 7. The S-Parameters for MIMO system a- S Parameters and b- mutual-coupling

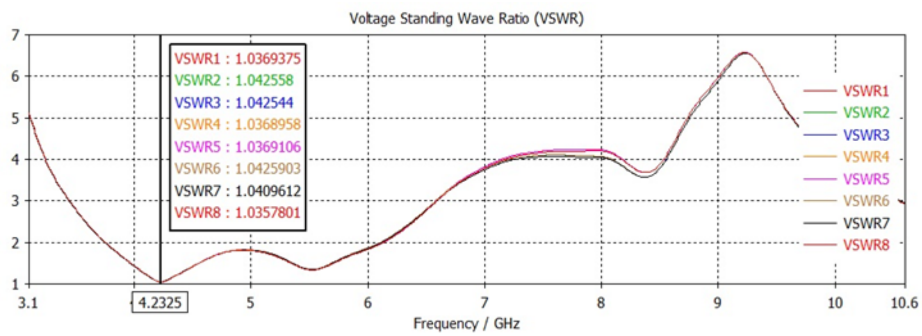

Fig. 8. VSER of suggested MIMO Antenna

An important measure is the Envelope Correlation Coefficient (ECC) which is taken into account when calculating the variety of an antenna's performance. They are employed to determine how similar two beam patterns are to one another. The two beam patterns may have less overlap as a result of the reduced correlation [22]. Can be used the following equation (1) [23] to determine the value of ECC:

$$\rho_e \frac{|S_{11} \times S_{12} + S_{21} \times S_{22}|}{|(1-|S_{11}|^2-|S_{21}|^2)(1-|S_{22}|^2-|S_{12}|^2)|} \tag{1}$$

Fig. 9 displays the findings of the suggested antenna's correlation coefficient, which was less than 0.0001 at its operating frequency. It demonstrates that such a coefficient is far below the median value (0.5) [24].

The second important parameter that shows the antenna efficiency in terms of the diversity gain set is called diversity gain (DG). Using equation (2) [23], the outcomes are calculated and shown in Fig. 10:

$$DG = \sqrt{1} - ECC^2 \tag{2}$$

About the radiation pattern, the 2D polar pattern for all ports which appears omnidirectional is displayed in Fig. 11 with lobes having an angular width of 41.8 degrees. Add to that, the H-max and gain for the coverage area for the 3D pattern employing all ports simultaneously are -32.03 dB and 6.442 dBi, respectively.

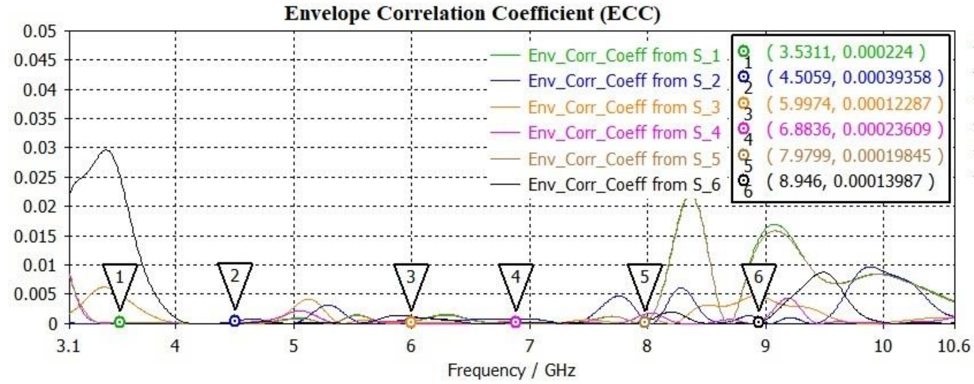

Fig. 9. Details of ECC for MIMO antenna

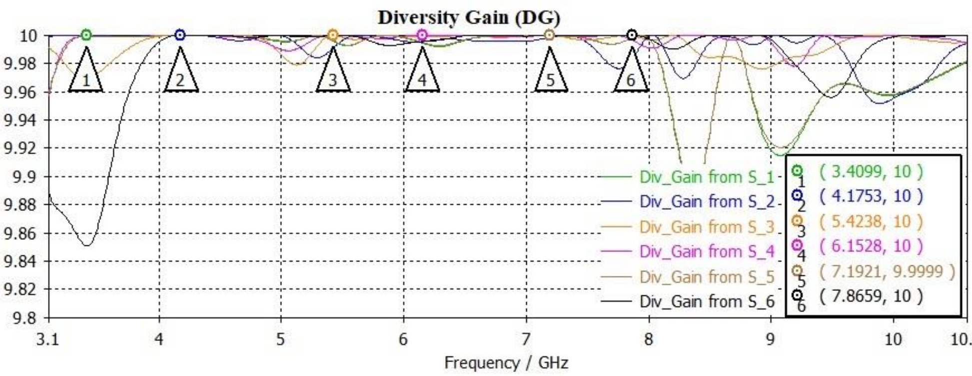

Fig. 10. Details of DG for MIMO antenna

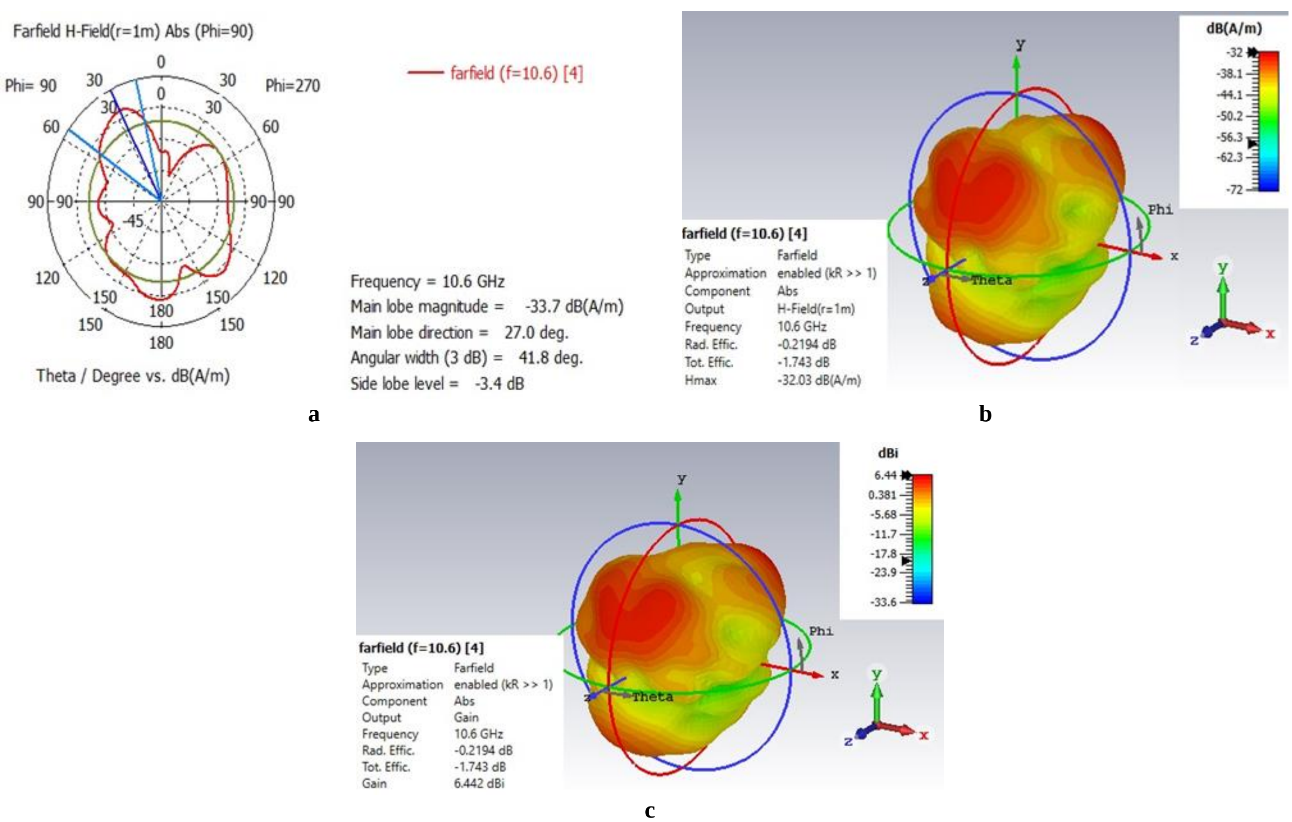

Fig. 11. Radiation Pattern of the MIMO Antenna System a-2D, b- 3D, and c- Gain

Finally, the suggested ports of the antenna are shown in Fig. 12 from the modelling of 3D radiation pattern performances. It demonstrates that each side of the design can be covered by the radiation patterns of radiators. Due to the dual-polarized features of the antenna component, various polarizations may be accomplished simultaneously for each PCB region, hence making the proposed MIMO antenna system appropriate for future mobile applications.

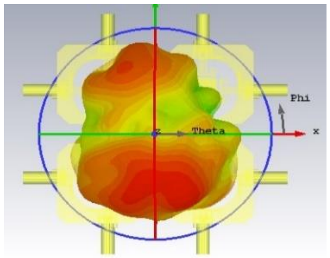

Antenna.1

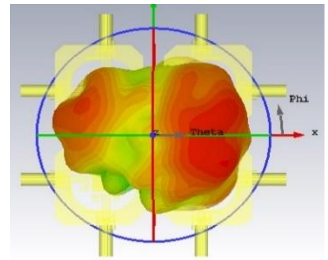

Antenna.2

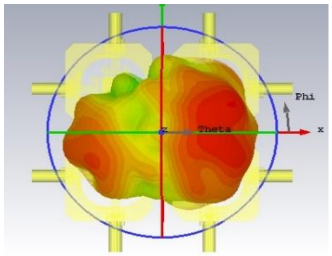

Antenna.3

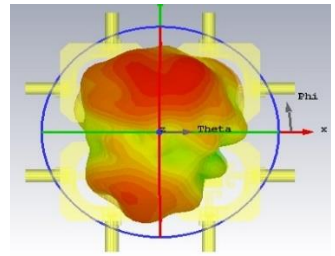

Antenna.4

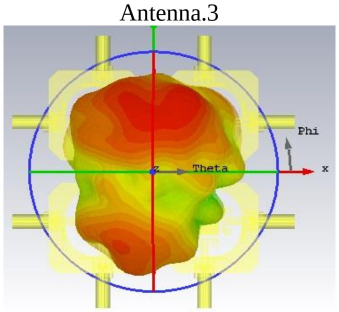

Antenna.5

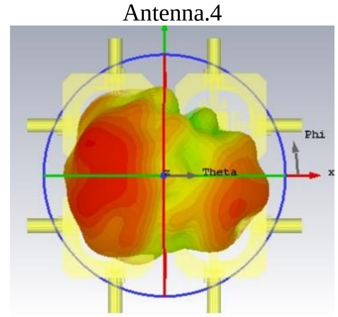

Antenna.6

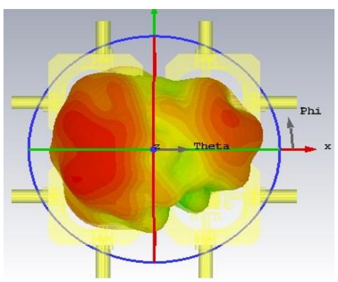

Antenna.7

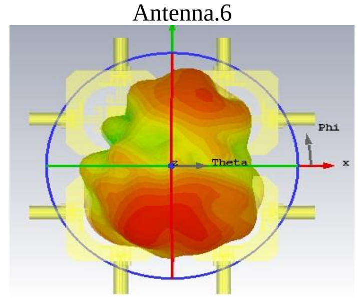

Antenna.8

Fig. 12. Three-dimensional radiation patterns for MIMO antenna

Table 2 contrasts the data presented in this research for different parameters with some comparable findings reported by other authors.

Table 2. Comparing the outcomes of some works

References	Publication Year	Port no.	Design size (mm)	Bandwidth (GHz)	Gain (dB)	VSWR dB	DG	ECC	Efficiency %
[25]	2019	8	150 ×75	0.6	5	doesn't approach 2	Did not mention	0.5	60%
[25]	2020	8	155 × 85	0.59	4.85	doesn't approach 2	Did not mention	Did not mention	Did not mention
[26]	2020	8	139 × 67	0.85	5.514	doesn't approach 2	approach 10	0.001	Did not mention
[27]	2019	8	150 × 75	0.6	Did not mention	Did not mention	Did not mention	0.01	71%
My design	2023	8	64.59 × 64.59	2.33	6.442	1.03	10	0.0001	97%

4. Conclusion

A CP dual-polarized antenna design for a MIMO system is discussed in this research. The antenna schematic consists of four components, each with a dual-port and four Umbrella-shaped microstrip feed lines positioned at the corners of a (64.59 x 64.59) mm^2 PCB. Without the use of decoupling techniques, polarization diversity is provided by the orthogonal orientation of the antenna's microstrip feed lines with a very low correlation coefficient. High impedance matching (about -59.6 dB reflection coefficients) is attainable by varying the length and breadth of microstrip feed lines. The final proposed MIMO prototype indicates that the single element operates at 4.25 GHz and covers 2.36 GHz (3.78

GHz-6.14 GHz) at -10dB while MIMO running at 4.23 GHz with a bandwidth of 2.33 GHz (3.77 - 6.1) GHz at -10dB. The findings demonstrated the recommended antenna's advantageous qualities and meet the needs of emerging device applications.

Acknowledgements

Sincere gratitude and appreciation are due to the Middle Technical University for all of their help, which was essential to the completion and advancement of this scientific achievement.

Reference

[1] A. G. Ferreira, D. Fernandes, A. P. Catarino, and J. L. Monteiro, “Performance analysis of ToA-based positioning algorithms for static and dynamic targets with low ranging measurements,” Sensors (Switzerland), vol. 17, no. 8, pp. 9–11, 2017, doi :10.3390/s17081915.
[2] M. A. Nizar, “A Microstrip Wireless Antenna Used By Capsule For Stomach Internal Photography,” J. Tech., vol. 1, no. 1, pp. 30–38, 2020, doi: 10.51173/jt.v1i1.62.
[3] C. Chinabutr and S. Promwong, “Evaluation of UWB antennas at 7-9 GHz for short range wireless communications,” 3rd Int. Conf. Digit. Arts, Media Technol. ICDAMT 2018, doi: 10.1109/ICDAMT.2018.8376529.
[4] R. Based, “Positioning and Tracking of Multiple Humans Moving in Small,” 2022, doi: 10.3390/s22145228.
[5] A. Joshi and R. Singhal, “Gain enhancement in probe-fed hexagonal ultra wideband antenna using AMC reflector,” J. Electromagn. Waves Appl., vol. 33, no. 9, pp. 1185–1196, 2019, doi: 10.1080/09205071.2019.1605939.
[6] D. A. Bashar, “Artificial Intelligence Based LTE MIMO Antenna for 5th Generation Mobile Networks,” J. Artif. Intell. Capsul. Networks, vol. 2, no. 3, pp. 155–162, 2020, doi: 10.36548/jaicn.2020.3.002.
[7] T. Addepalli and V. R. Anitha, “A very compact and closely spaced circular shaped UWB MIMO antenna with improved isolation,” AEU - Int. J. Electron. Commun., vol. 114, p. 153016, 2020, doi: 10.1016/j.aeue.2019.153016.
[8] Y. Niu, Y. Li, D. Jin, L. Su, and A. V. Vasilakos, “A survey of millimeter wave communications (mmWave) for 5G: opportunities and challenges,” Wirel. Networks, vol. 21, no. 8, pp. 2657–2676, 2015, doi: 10.1007/s11276-015-0942-z.
[9] M. A. Jensen and J. W. Wallace, “A review of antennas and propagation for MIMO wireless communications,” IEEE Trans. Antennas Propag., vol. 52, no. 11, pp. 2810–2824, 2004, doi: 10.1109/TAP.2004.835272.
[10] J. C. Coetzee and Y. Yu, “Design of decoupling networks for circulant symmetric antenna arrays,” IEEE Antennas Wirel. Propag. Lett., vol. 8, pp. 291–294, 2009, doi: 10.1109/LAWP.2008.2010566.
[11] C. Y. Chiu, C. H. Cheng, R. D. Murch, and C. R. Rowell, “Reduction of mutual coupling between closely-packed antenna elements,” IEEE Trans. Antennas Propag., vol. 55, no. 6, pp. 1732–1738, 2007, doi: 10.1109/TAP.2007.898618.
[12] N. O. Parchin et al., “Eight-Element Dual-Polarized MIMO Slot Antenna System for 5G Smartphone Applications,” IEEE Access, vol. 7, pp. 15612–15622, 2019, doi: 10.1109/ACCESS.2019.2893112.
[13] Y. Ban, Z. Chen, Z. Chen, K. Kang, and J. L. Li, “Decoupled Hepta-Band Antenna Array for,” vol. 13, pp. 999–1002, 2014, doi: 10.1109/LAWP.2014.2325877.
[14] A. S. Abdullah, S. A. Hashem, and M. F. Mosleh, “A Design of CP-MIMO System with Elements of a Diamond-Ring Slot for 5G Mobile-Phone,” J. Tech., vol. 3, no. 2, pp. 53–60, 2021, doi: 10.51173/jt. v3i2.334.
[15] N. O. Parchin et al., “Eight-Element Dual-Polarized MIMO Slot Antenna System for 5G Smartphone Applications,” IEEE Access, vol. 7, pp. 15612–15622, 2019, doi: 10.1109/ACCESS.2019.2893112.
[16] N. O. Parchin, Y. I. A. Al-Yasir, H. J. Basherlou, R. A. Abd-Alhameed, and J. M. Noras, “Orthogonally dual-polarised MIMO antenna array with pattern diversity for use in 5G smartphones,” IET Microwaves, Antennas Propag., vol. 14, no. 6, pp. 457–467, 2020, doi: 10.1049/iet-map.2019.0328.
[17] A. Sharma, “A-shaped wideband dielectric resonator antenna for wireless communication systems and its MIMO implementation,” no. January, 2018, doi: 10.1002/mmce.21402.
[18] A. K. Biswas and U. Chakraborty, “Reduced mutual coupling of compact MIMO antenna designed for WLAN and WiMAX applications,” Int. J. RF Microw. Comput. Eng., vol. 29, no. 3, pp. 13–20, 2019, doi: 10.1002/mmce.21629.
[19] N. Hussain, M. J. Jeong, A. Abbas, and N. Kim, “Metasurface-Based Single-Layer Wideband Circularly Polarized MIMO Antenna for 5G Millimeter-Wave Systems,” IEEE Access, vol. 8, pp. 130293–130304, 2020, doi: 10.1109/ACCESS.2020.3009380.
[20] R. V. S. R. Krishna and R. Kumar, “Design and investigations of a microstrip fed open V-shape slot antenna for wideband dual slant polarization,” Eng. Sci. Technol. an Int. J., vol. 18, no. 4, pp. 513–523, 2015, doi: 10.1016/j.jestch.2015.03.005.
[21] R. V. R. Krishna, R. Kumar, and N. Kushwaha, “An UWB dual polarized microstrip fed L-shape slot antenna,” Int. J. Microw. Wirel. Technol., vol. 8, no. 2, pp. 363–368, 2016, doi: 10.1017/S1759078715000124.
[22] N. O. Parchin et al., “Mobile-phone antenna array with diamond-ring slot elements for 5G massive MIMO systems,” Electron., vol. 8, no. 5, pp. 1–17, 2019, doi: 10.3390/electronics8050521.
[23] A. H. Jabire, H. X. Zheng, A. Abdu, and Z. Song, “Characteristic mode analysis and design of wide band MIMO antenna consisting of metamaterial unit cell,” Electron., vol. 8, no. 1, 2019, doi: 10.3390/electronics8010068.
[24] S. Saxena, B. K. Kanaujia, S. Dwari, S. Kumar, and R. Tiwari, “A Compact Dual-Polarized MIMO Antenna with Distinct Diversity Performance for UWB Applications,” IEEE Antennas Wirel. Propag. Lett., vol. 16, no. c, pp. 3096–3099, 2017, doi: 10.1109/LAWP.2017.2762426.
[25] N. O. Parchin et al., “Eight-Element Dual-Polarized MIMO Slot Antenna System for 5G Smartphone Applications,” IEEE Access, vol. 7, pp. 15612–15622, 2019, doi: 10.1109/ACCESS.2019.2893112.
[26] N. Al-Ani, O. Al-Ani, M. Mosleh, and R. Abd-Alhameed, “Design a Four Dual polarizations MIMO System Based a Serrated Chord with Right Angle Triangle Shape,” 2020, doi: 10.7716/aem.v9i1.1333.
[27] X. Zhang, Y. Li, W. Wang, and W. Shen, “Ultra-Wideband 8-Port MIMO Antenna Array for 5G Metal-Frame Smartphones,” IEEE Access, vol. 7, pp. 72273–72282, 2019, doi: 10.1109/ACCESS.2019.2919622.